SEPARATION METHOD FOR CROSS-ALIASED NEAR-IR ABSORPTION LINES OF C_2H_4: A COAL SPONTANEOUS COMBUSTION MARKER**

Weifeng Wang [1,2*], Hanfei Liu [1,2], Gaoming Wei [1,2], Bo Yang [1,2], Lifeng Ren [1,2], Jun Li [1,2], Bao Liu [3]

[1] School of Safety Science and Engineering at Xi'an University of Science and Technology, Xi'an Shaanxi, China; e-mail: wangwf@xust.edu.cn; wgm20180326@163.com
[2] Key Laboratory of Mine and Disaster Prevention and Control of Ministry of Education at Xi'an University of Science and Technology, Xi'an Shaanxi, China
[3] College of Electrical and Control Engineering at Xi'an University of Science and Technology, Xi'an Shaanxi, China

To tackle the cross-interference problem between CH_4 and C_2H_4 and the aliasing interference problem of C_2H_4 itself, on the basis of the sparse decomposition theory, multiple Lorentz function-based methods were proposed for separating the cross-aliasing interference of near-infrared (IR) C_2H_4 absorption lines. A quadruple Lorentz function-based separation model describing the absorption coefficient of C_2H_4 is developed, with which the absorption lines of background gas and to-be-measured C_2H_4 were separated from the absorption lines of mixed gas, thereby effectively separating the absorption line of C_2H_4 and accurately measuring its concentration. The results show that the maximum errors of C_2H_4 and CH_4 gasometrical analyses are $5.3\times10^{-6}/201.7\times10^{-6}$ and $57\times10^{-6}/5000\times10^{-6}$, respectively. The proposed method effectively eliminates the errors caused by cross-aliasing interference of C_2H_4 absorption lines in the near-IR bands and improves the detection accuracy of the TDLAS gas detection system. The findings of this study provide a feasible solution to the cross-aliasing interference problem of IR absorption lines.

Keywords: *coal spontaneous combustion, representative gas, C_2H_4, absorption line, aliasing interference.*

МЕТОД РАЗДЕЛЕНИЯ ПЕРЕКРЫВАЮЩИХСЯ ЛИНИЙ ПОГЛОЩЕНИЯ C_2H_4 В БЛИЖНЕМ ИК-ДИАПАЗОНЕ КАК МАРКЕР САМОВОЗГОРАНИЯ УГЛЯ

W. Wang [1,2*], H. Liu [1,2], G. Wei [1,2], B. Yang [1,2], L. Ren [1,2], J. Li [1,2], B. Liu [3]

УДК 535.34:(547.313.2+547.211)

[1] Школа науки и техники безопасности Сианьского университета науки и техники, Сиань, Шэньси, Китай; e-mail: wangwf@xust.edu.cn; wgm20180326@163.com
[2] Главная лаборатория по борьбе со стихийными бедствиями Министерства образования Сианьского университета науки и техники, Сиань, Шэньси, Китай
[3] Колледж электротехники и систем управления Сианьского университета науки и техники, Сиань, Шэньси, Китай

(Поступила 1 июня 2022)

Для решения проблем перекрестной интерференции между CH_4 и C_2H_4 и интерференции линий C_2H_4 в ближнем ИК-диапазоне разработана основанная на функции Лоренца модель разделения, описывающая коэффициент поглощения C_2H_4, с помощью которой линии поглощения фонового газа и подлежащего измерению C_2H_4 отделены от линий поглощения газовой смеси. Таким образом выделена линия поглощения и точно измерена концентрация C_2H_4. Максимальные погрешности газометрического анализа C_2H_4 и CH_4 $5.3\times10^{-6}/201.7\times10^{-6}$ и $57\times10^{-6}/5000\times10^{-6}$. Предлагаемый

**Full text is published in JAS V. 90, No. 1 (http://springer.com/journal/10812) and in electronic version of ZhPS V. 90, No. 1 (http://www.elibrary.ru/title_about.asp?id=7318; sales@elibrary.ru).

способ эффективно устраняет ошибки, вызванные перекрестной интерференцией линий поглощения C_2H_4 в ближнем ИК-диапазоне, и повышает точность системы обнаружения газа TDLAS.

Ключевые слова: *самовозгорание угля, репрезентативный газ, C_2H_4, линия поглощения, интерференция.*

Introduction. Risk determination of coal spontaneous combustion, which causes a significant loss of coal resources and environmental pollution every year, is a worldwide technical challenge. During coal oxidation heating, ethylene (C_2H_4) can serve as a sensitive indicator for ignition characterization of low-metamorphic coal in gasometrical analysis, which can also be used as an indicator for the degree of coal spontaneous combustion and extinction. Thus, fast and accurate monitoring of C_2H_4 is very important. With high sensitivity, non-intrusive nature, and selectivity, tunable diode laser absorption spectroscopy (TDLAS) technology allows simultaneous detection of multiple gases, which has prominent advantages in the accurate detection of coal spontaneous combustion marker gases. Coal spontaneous combustion disasters spread across the world, not only causing a significant loss of coal resources and environmental pollution every year but also seriously threatening the ecosystem and human health, which has become a global disaster [1–3]. Unlike other types of solid fires, coal spontaneous combustion is characterized by self-ignition, smoldering, and re-ignition, which is extremely difficult to prevent and control because of the concealed fire source [4, 5], oxygen-deficient oxidation, and easy re-ignition. Risk determination of coal spontaneous combustion is a worldwide challenge [6, 7], and much in-depth research has been conducted from different perspectives by numerous scholars across the world. Given the poor thermal conductivity of coal, gas detection has recently been adopted to determine the risk level of coal spontaneous combustion [8, 9]. During coal oxidation, heat is continuously accumulated and a series of gaseous components, including CO, C_2H_6, CH_4, C_2H_4, and C_2H_2, are released [10, 11]. The release duration, concentrations, and types of these gases correlate with the type of coal, geological conditions, temperature, oxygen concentration, etc. Different types of coals release different types of gas during oxidation, whereas the temperature and time differences vary when the gases are released. Hence, for accurate prediction of coal spontaneous combustion, it is crucial to select a reasonable gas that can reflect the temperature and state of combustion. To improve the accuracy and sensitivity of prediction, the C_2H_4 or C_2H_4/C_2H_2 ratio is often used in combination with gas indicators such as CO, by which the state of coal spontaneous combustion can be accurately determined [12]. C_2H_4, emerges later than CO, which is detectable at around 110°C; hence, it can be recognized as a marker gas for the accelerated oxidation stage of the coal spontaneous combustion process [13]. It can serve as a sensitive indicator for ignition characterization of low-metamorphic coal in gasometrical analysis, which can also be used as an indicator for the degree of coal spontaneous combustion and extinction. By monitoring the concentration of C_2H_4, coal spontaneous combustion can be forecast. Once the indicator gas exceeds the threshold, timely treatments should be taken to prevent further spontaneous combustion.

As a new approach to high-sensitivity gas detection, TDLAS technology has advantages of noncontact, high selectivity, high sensitivity, fast response, high efficiency, long calibration period, and capability for dynamic detection [14, 15], which allows simultaneous detection of multiple gases [16, 17]. Thus, TDLAS are promising for the accurate detection of C_2H_4 as a coal spontaneous combustion marker gas. Detecting the C_2H_4 composition, concentration, and change rates during spontaneous combustion by using TDLAS technology provides reliable data for early combustion warning and relevant risk level determination, which has significant research value.

Extensive basic studies have been conducted concerning TDLAS technology across the world [18–20], which are valuable for application in industrial safety monitoring, environmental monitoring, etc. However, simultaneous trace detections of coal spontaneous combustion marker gases based on TDLAS technology have not yet been reported. As is clear from Fig. 1, the detection accuracy is limited by the cross-interference between CH_4 and C_2H_4, the serious aliasing interference of absorption lines of C_2H_4 itself, and the poor single-peak feature of C_2H_4 near-IR absorption lines. Hence, high-precision TDLAS detection of C_2H_4 can be achieved by tackling the cross-interference problem between CH_4 and C_2H_4, as well as the aliasing interference problem of C_2H_4 absorption lines. In this paper, focusing on the aforementioned problems, we propose multiple Lorentz function-based methods for separating the cross-aliasing interference of C_2H_4 near-IR absorption lines, to effectively separate the absorption lines of C_2H_4 and accurately measure its concentration.

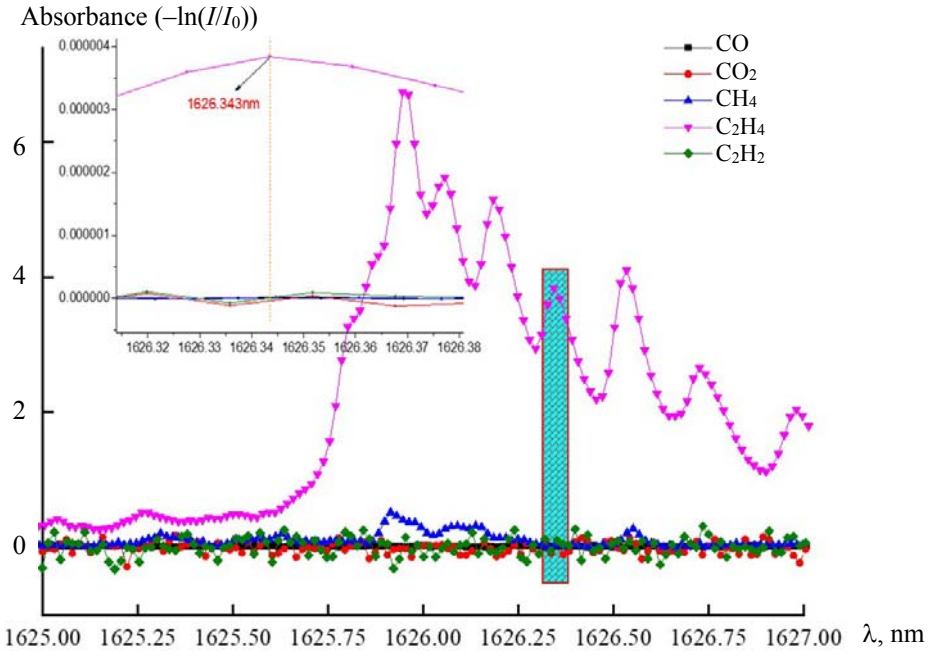

Fig. 1. Absorption line distribution of C_2H_4 at the 1626.343 nm central wavelength.

Beer–Lambert law. Attenuation of IR spectral intensity caused by the absorption of gas molecules is related to the optical path length of light passing through the target gas and the concentration of the target gas, which can be described by the Beer–Lambert law [21, 22] with an expression of:

$$A(\nu) = -\ln\frac{I_0(\nu)}{I(\nu)} = \alpha(\nu)CL\,, \tag{1}$$

where $I_0(\nu)$ and $I(\nu)$ represent incident and outgoing light intensities; ν represents the wave number, $\nu = 1/\lambda$; $\alpha(\nu)$ represents the absorption coefficient of the target gas; $A(\nu)$ represents the absorbance; C represents the volume concentration of target gas per unit pressure; L represents the total optical path of light passing through the target gas. According Eq. (1), if the light intensity of incident light and the total optical path passing through the target gas are determined, the target gas concentration can be derived directly from the attenuation of light intensity. The expression for the target gas concentration is:

$$C = \frac{A(\nu)}{S(T)PL}\,, \tag{2}$$

where $S(T)$ denotes the absorption line intensity of the gas spectral line per unit pressure, $cm^{-2} \cdot atm^{-1}$; T represents the temperature, °C; P denotes the ambient pressure of target gas, atm.

Experimental system. To test the method we proposed, we built an experimental system for the gas contraction calibration based on a commercialized high-precision gas distribution device, as shown in Fig. 2. The gas distribution mode is the flowed distribution mode, and the flow rate of each channel can be set via computer software. By using this system, we can produce a gas mixture with eight components and control the concentration of each component with a ppv-level accuracy. During the experimental characterization, the Herriott cell is first purged by pure nitrogen gas for 5 min to avoid the interference of residual gas in the cell, and then is fulfilled by the tested gas with pre-set concentration. The intensity of the optical signal passing the Herriott cell is collected by a focusing lens and detected by a photodetector, which is connected to the computer via a lock-in amplifier.

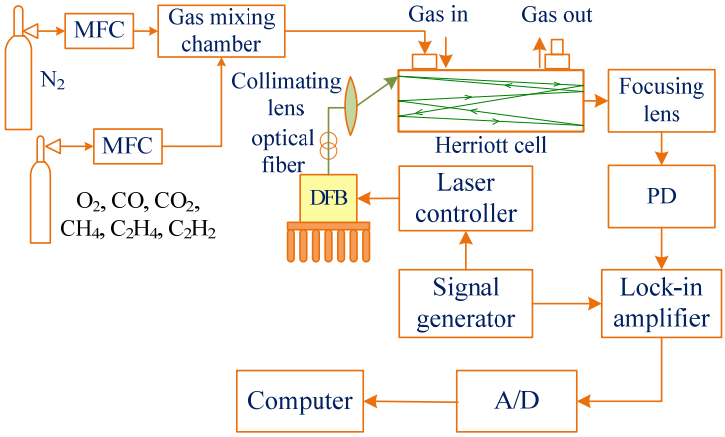

Fig. 2. Experimental system for gas concentration calibration.

Multiple Lorentz decompositions for separating cross-aliased C_2H_4 absorption lines. With the presence of multi-component absorption gases in the vicinity of the absorption line of the target gas, the Beer–Lambert absorption law can be rewritten as:

$$A(\nu) = \ln[I_0(\nu)/I_t(\nu)] = [\alpha_1(\nu)C_1 + \alpha_2(\nu)C_2 + \cdots + \alpha_n(\nu)C_n]L\,. \quad (3)$$

Equation (3) can be excessively described as:

$$A(\nu) = \ln I_0(\nu) - \ln I_t(\nu) = \alpha_1(\nu)C_1L + \alpha_2(\nu)C_2L\cdots + \alpha_n(\nu)C_nL\,, \quad (4)$$

where ν denotes the laser frequency; $I_0(\nu)$ and $I_t(\nu)$ denote the incident and outgoing light signals, respectively; $A(\nu)$ represents the absorbance of gas; $\alpha(\nu)$ represents the gas absorption coefficient; C is the gas concentration; and L is the optical path length.

The Beer–Lambert absorption law commonly used in TDLAS is expressed as:

$$A(\nu) = \ln I_0(\nu) - \ln I_t(\nu) = S(T)pg(\nu)CL\,, \quad (5)$$

where $S(T)$ stands for the absorption line intensity; p denotes the gas pressure; $g(\nu)$ is the Lorentzian line shape. The expression for $g(\nu)$ is:

$$g(\nu) = d/\pi\frac{1}{(\nu-\nu_0)^2 + d^2}\,, \quad (6)$$

where d denotes the collisional broadening half-width.

By combining Eqs. (1), (5), and (6), we can derive the expression of the gas absorption coefficient, which can be given as:

$$\alpha(\nu) = S(T)pg(\nu) = \frac{S(T)pd/\pi}{(\nu-\nu_0)^2 + d^2}\,. \quad (7)$$

Near the absorption line at 1626 nm, the absorption line of C_2H_4 is primarily cross-overlapped with that of CH_4. As clearly shown in Fig. 3, the cross-overlap interference of CH_4 exists at the positions where the four strongest absorption peaks occur. Because under normal conditions, the concentration of CH_4 is at least 2 orders of magnitude higher than that of C_2H_4, the absorption lines at these wavelengths are greatly influential to the C_2H_4 measurements. Based on these facts, the peak at 1626.343 nm was selected as the optimal absorption line of C_2H_4.

Within the absorption band 1626.0–1626.6 nm, C_2H_4 has four different absorption peaks. Thus, the Lorentz line-shape functions can be used to represent the relevant absorption coefficients. Besides, the central wavelengths and line widths of the Lorentz line-shape functions at these four peaks are relatively stable, which are immune to the variation of C_2H_4 concentration. Hence, a quadruple Lorentz function model are developed to describe the C_2H_4 absorbance, which can be given as:

$$M(\nu, s_1, s_2, s_3, s_4) = \frac{s_1}{(\nu-\nu_1)^2 + \alpha_1^2} + \frac{s_2}{(\nu-\nu_2)^2 + \alpha_2^2} + \frac{s_3}{(\nu-\nu_3)^2 + \alpha_3^2} + \frac{s_4}{(\nu-\nu_4)^2 + \alpha_4^2}\,, \quad (8)$$

where $\nu_1 = 1626.057$ nm, $\alpha_1 = 0.04484$ nm, $\nu_2 = 1626.184$ nm, $\alpha_2 = 0.0434$ nm, $\nu_3 = 1626.343$ nm, $\alpha_3 = 0.04421$ nm, $\nu_4 = 1626.535$ nm, $\alpha_4 = 0.04502$ nm, and s refers to the undetermined coefficients associated with absorption peaks.

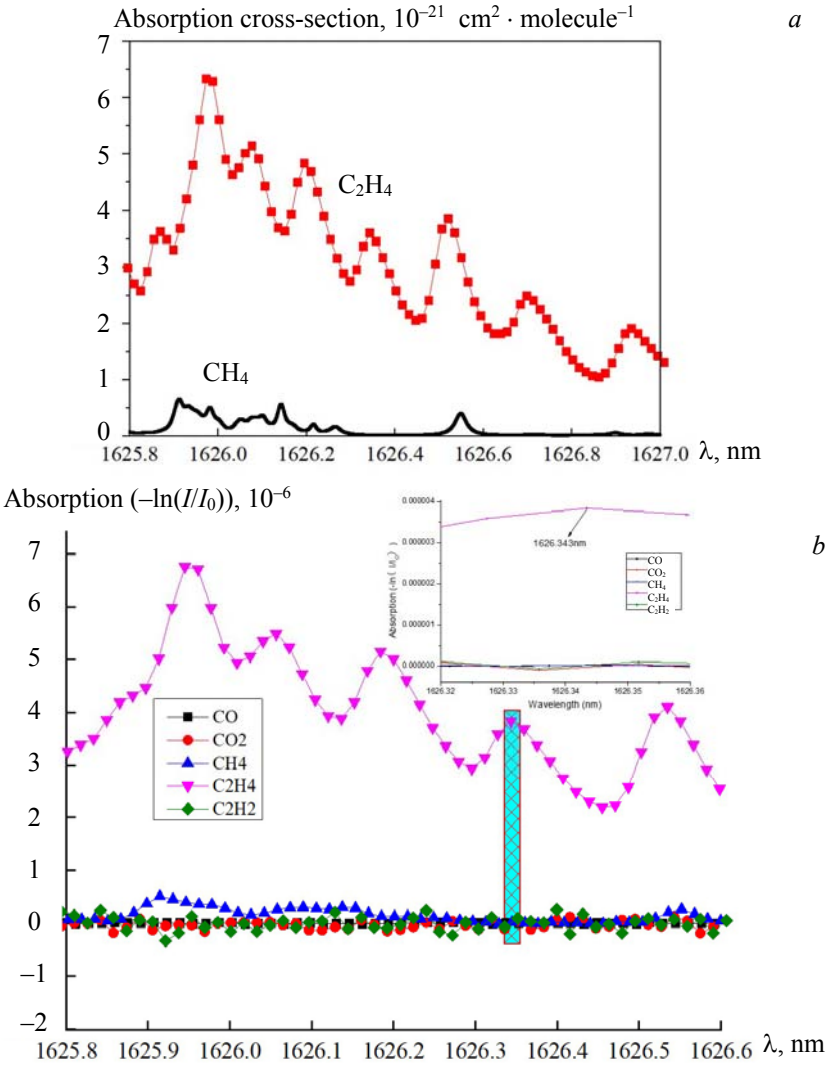

Fig. 3. Cross-section (a) absorption and (b) absorbance values of CH_4 and C_2H_4 around near-IR 1626 nm.

According to Eq. (7):

$$s_i = S_i(T)pC_{C_2H_4}L\,. \tag{9}$$

When the temperature T, pressure p, and optical length L are known, the C_2H_4 concentration can be inverted through multiple Lorentz fitting.

Cross-aliasing interference between CH_4 and C_2H_4 is mainly considered during the detection of C_2H_4 in multi-component gases from coal spontaneous combustion. Accordingly, the following equation can be derived from Eq. (4):

$$\ln I_0(\nu) - \ln I_t(\nu) = [M(\nu, s_1, s_2, s_3, s_4) + D\alpha_{\text{methane}}(\nu)], \tag{10}$$

where $M(\nu, s_1, s_2, s_3, s_4)$ denotes the absorbance of C_2H_4; $D\alpha_{\text{methane}}(\nu)$ is the absorbance of CH_4. According to Eq. (4), the concentration-associated undetermined coefficient D is:

$$D = C_{CH_4}L\,. \tag{11}$$

Through nonlinear fitting of Eq. (10) by the least square method, various undetermined coefficients were obtained, thereby achieving separation of the target gas and background absorption lines from the mixed gas absorption line. Based on the calibration results of undetermined coefficients and gas concentrations, $C_{C_2H_4}$ (concentration of C_2H_4) and C_{CH_4} (concentration of CH_4) were obtained. To assess the effect of the quadruple Lorentz decomposition in separating the multi-component gases from coal spontaneous combustion, two groups of standard mixed gases, namely sample gas 1 and sample gas 2, were assigned. Table 1 lists the

components and concentrations of the two sample gases, where the carrier gas is nitrogen. The standard mixed gases mainly comprised the atmospheric air and the gases generated by coal spontaneous combustion and oxidation.

TABLE 1. Components and Concentrations of Two Sample Gases

Standard 1 gas composition	Concentration, %	Standard 2 gas composition	Concentration, %
CO	102.4×10^{-6}	CO	199.2×10^{-6}
CO_2	501.6×10^{-6}	CO_2	0.5
CH_4	0.5	CH_4	0.5
C_2H_4	99.2×10^{-6}	C_2H_4	201.7×10^{-6}
C_2H_2	31.9×10^{-6}	C_2H_2	58.3×10^{-6}
O_2	18	O_2	12

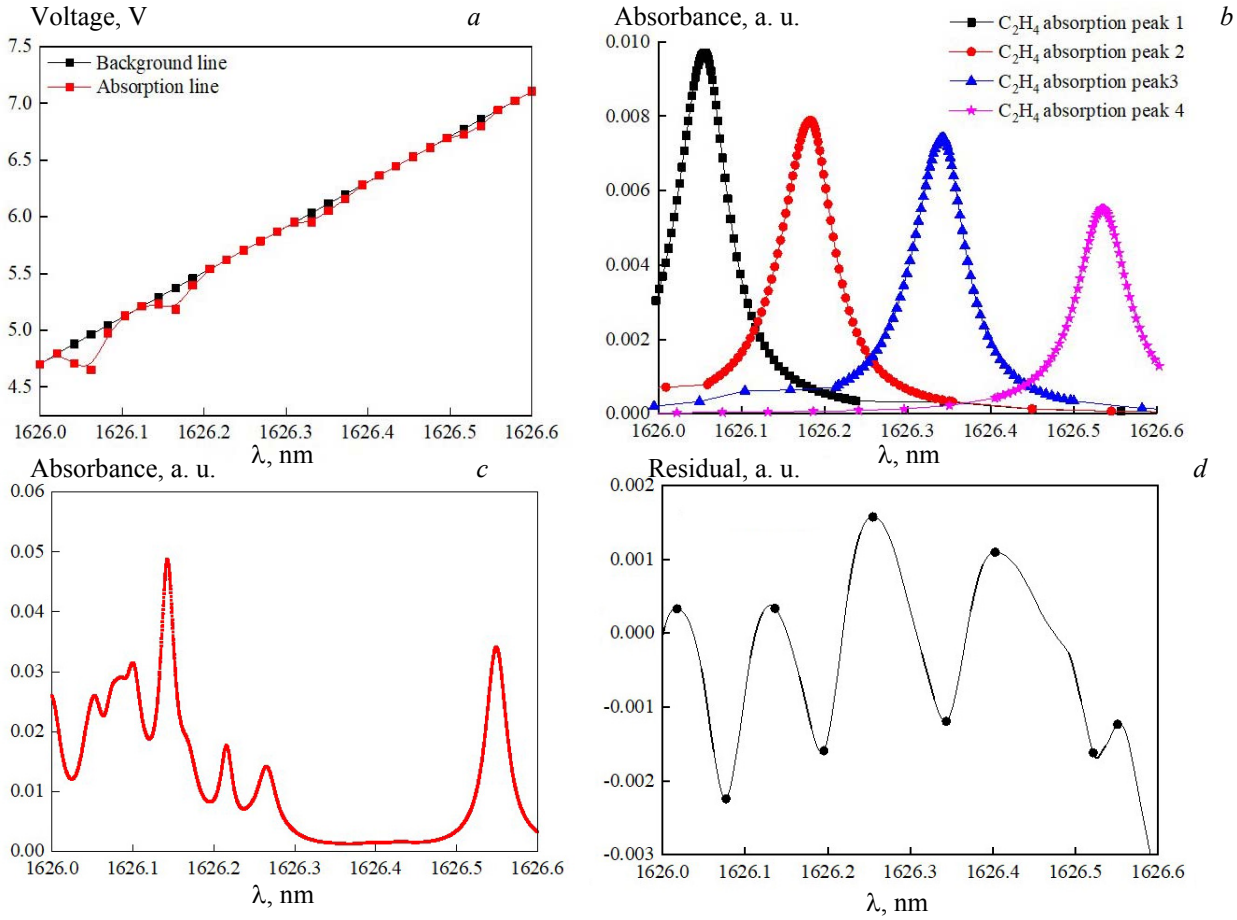

Fig. 4. Absorption line separation effect with standard samples gas 1: (a) Absorption and background lines, (b) C_2H_4 absorption peaks, (c) CH_4 absorption peaks, and (d) Residual.

To measure the standard sample gas 1, different concentrations of multi-component standard gases from coal spontaneous combustion were prepared using high-purity (99.999%) nitrogen as the carrier gas. According to the sparse decomposition theory, the scanning absorption lines of to-be-measured gas were decomposed, and the absorption lines of target gas were separated by the quadruple Lorentz decomposition method. Figure 4 displays the absorption line separation results with the C_2H_4 concentration of 59.52×10^{-6}. Next, the corresponding gas concentrations were inverted based on the separated C_2H_4 and CH_4 absorption lines, respectively. Table 2 lists different concentrations of C_2H_4 and CH_4 obtained with the standard sample gas 1, as well as their detection results. According to the data in Table 2, the maximum detection error of C_2H_4 concentration using standard sample gas 1 can be evaluated as 4.22×10^{-6}, whereas that of CH_4 concentration is 46×10^{-6}.

TABLE 2. Different Concentrations of C_2H_4 and CH_4 were Obtained Using Standard Sample Gas 1 and Gas 2 and their Detection Results

Flow, L/min	Proportioning concentration, 10^{-6}			Measure concentration, 10^{-6}		Error, 10^{-6}	
Gas 1							
N_2 (99.999%)	Standard gas 1	C_2H_4	CH_4	C_2H_4	CH_4	C_2H_4	CH_4
0.8	0.2	19.84	1000	21.6	976	1.76	−24
0.6	0.4	39.68	2000	37.2	2015	−2.48	15
0.4	0.6	59.52	3000	55.3	3029	−4.22	29
0.2	0.8	79.36	4000	83.4	3967	4.04	−33
0	1	99.20	5000	95.7	5046	−3.50	46
Gas 2							
0.8	0.2	40.34	1000	42.9	971	2.56	−29
0.6	0.4	80.68	2000	78.1	2042	–2.58	42
0.4	0.6	121.02	3000	116.5	2983	–4.52	−17
0.2	0.8	161.36	4000	166.6	3943	5.24	−57
0	1	201.7	5000	195.4	4955	–5.3	−45

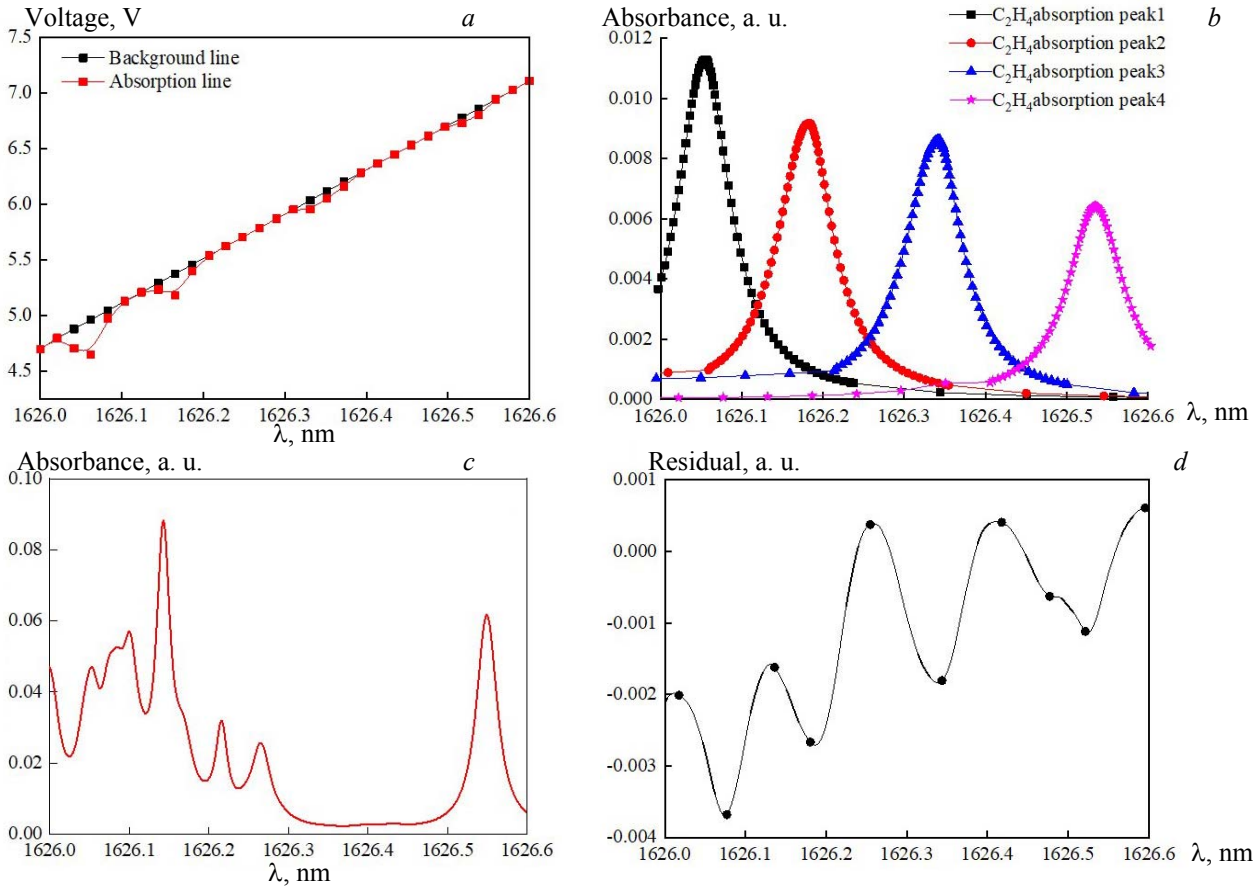

Fig. 5. Absorption line separation effect with standard samples gas 2: (a) Absorption and background lines, (b) C_2H_4 absorption peaks, (c) CH_4 absorption peaks, and (d) Residual.

Standard sample gas 2 was experimentally measured in the similar way, where different concentrations of multi-component gases from coal spontaneous combustion were prepared using the gas mixing system. Table 2 lists the relevant C_2H_4 and CH_4 concentrations. The absorption lines of the target gas were separated by using the quadruple Lorentz decomposition method. Figure 5 shows the absorption line separation results with the C_2H_4 concentration of 80.68×10^{-6}. Thereafter, the corresponding gas concentrations were inverted using the separated C_2H_4 and CH_4 absorption lines, respectively. Table 2 lists different concentrations of C_2H_4 and CH_4 obtained with the standard sample gas 2, as well as their detection results. According to the

data in the table, the maximum detection error of C_2H_4 concentration using standard sample gas 2 is $5.3\times10^{-6}/201.7\times10^{-6}$, whereas that of CH_4 concentration is $57\times10^{-6}/5000\times10^{-6}$.

As suggested by the above experimental results, the quadruple Lorentz decomposition allows separation of the C_2H_4 and CH_4 absorption lines from multi-component coal spontaneous combustion gases and enables accurate concentration detection of the two gases. Within the spectral scanning band of 1626.0–1626.6 nm, the C_2H_4 absorption line in multi-component coal spontaneous combustion gases is interfered with primarily by the cross-aliasing of absorption lines, whereas the interference of other gases is negligible. The measured concentration of CH_4 in the multi-component standard mixed gas is more than 20 times higher than that of C_2H_4. The purpose is to provide strong interference of CH_4 absorption lines for the measurement of C_2H_4 concentration and to thereby examine the effect of the quadruple Lorentz decomposition method. The measurement data show that the maximum error of this separation method for measuring C_2H_4 concentration is $5.3\times10^{-6}/201.7\times10^{-6}$, whereas that for measuring CH_4 concentration is $57\times10^{-6}/5000\times10^{-6}$, suggesting that the proposed method can meet the requirements of actual detection.

Conclusions. Focusing on the cross-interference issues between CH_4 and C_2H_4, as well as the aliasing interference problem of C_2H_4 absorption lines, multiple Lorentz function-based methods for separating the cross-aliasing interference of C_2H_4 near-IR absorption lines are proposed according to the sparse decomposition theory. A quadruple Lorentz function-based separation model describing the absorption coefficient of C_2H_4 is developed. With the multiple Lorentz decompositions, a quadruple Lorentz function-based decomposition model is used to describe the C_2H_4 absorption coefficient, and the absorption lines of to-be-measured C_2H_4 and background CH_4 are separated from the cross-aliased absorption lines of the target gas, thereby separating the overlapped absorption lines of C_2H_4 and CH_4, as well as the aliased absorption lines of C_2H_4 itself. The maximum error of C_2H_4 gasometrical analysis is $5.3\times10^{-6}/201.7\times10^{-6}$, whereas that of the concentration of CH_4 gasometrical analysis is $57\times10^{-6}/5000\times10^{-6}$. The experimental results show that the proposed multiple Lorentz function-based separation method can effectively eliminate the cross-aliasing interference of C_2H_4 absorption lines in the near-IR bands, reduce the measurement errors, and improve the detection accuracy and stability of the TDLAS gas detection system.

Acknowledgments. This work was supported by the National Key R & D Plan of China (No. 2021YFE0105000), the National Natural Science Foundation of China (No. 52074213), Shaanxi Key R & D Plan Project (Nos. 2021SF-472 and 2021GY-131), Yulin Science and Technology Plan Project (Nos. CXY-2020-036 and CXY-2020-037), Science and Technology Fund for outstanding young people of Xi'an University of Science and Technology (No. 2019YQ2-01), Xi'an Science and Technology Plan Project (No. 2020KJRC0068).

REFERENCES

1. K. Brown, *Science*, **299**, 1177 (2003).
2. B. Qin, X. Zhong, D. Wang, et al., *Coal Sci. Technol*., **49**, 66–99 (2011).
3. J. Deng, Z. Bai, M. Xiao, et al., *Coal Mine Safety*, **51**, 118–125 (2020).
4. B. Du, Y. Liang, F. Tian, *Fire Safety J*., **121**, 103298 (2021).
5. Y. Wang, X. Li, Z. Guo, *Heat Transfer Res*., **49**, 827–845 (2018).
6. B. Demir, O. Oren, C. Sensogut, *Arab. J. Geosci*., **13**, 730 (2020).
7. L. Ma, R. Guo, M. Wu, et al., *Proc. Safety and Environ. Protection*, **142**, 370–379 (2020).
8. Y. Song, S. Yang, X. Hu, et al., *Proc. Safety and Environ. Protection*, **129**, 8–16 (2019).
9. Y. Wei, J. Chang, J. Lian, et al., *Photon. Sensors*, **5**, 67–71 (2015).
10. A. Dudzinska, *Fuel*, **246**, 232–243 (2019).
11. G. Wei, H. Wen, J. Deng, et al., *Fuel*, **284**, 119043 (2021).
12. H. Niu, X. Deng, S. Li, et al., *J. Central South University*, **23**, 2321–2328 (2016).
13. D. Zhang, X. Cen, W. Wang, et al., *Fuel*, **288**, 119635 (2021).
14. D.·G. Park, J. H. Wang, C. Lee, *Clean Technol*., **25**, 316–323 (2019).
15. S.·G. Buckley, *Spectroscopy*, **33**, 26–29 (2018).
16. Z. Qu, O. Werhahn, V. Ebert, *Appl. Spectrosc*., **72**, 853–862 (2018).
17. Q. Wang, P. Sun, Z. Zhang, et al., *ACTA Phys. Sin.*, **70**, 144203 (2021).
18. A. Sepman, Y. Ögren, Z. Qu, et al., *Proc. Comb. Institute*, **36**, 4541–4548 (2017).
19. N. Jeong, S. So, D. Kim, et al., *J. Energy Climate Change*, **15**, 128–141 (2020).
20. H. Chen, Y. Ju, L. Han, et al., *Spectrosc. Spectr. Anal.*, **41**, 1580–1585 (2021).
21. Z. Xin, J. Xing, *Spectrosc. Spectr. Anal.*, **37**, 2844–2848 (2017).
22. J. Jiang, M. Zhao, G. Ma, et al., *IEEE Sens. J*., **18**, 2318–2325 (2018).